J. Mol. Model. **1999**, *5*, 263 – 270

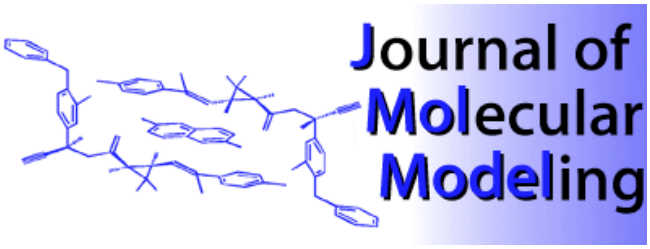

FULL PAPER

Three-Dimensional Analysis of CD6 Site-Directed Mutagenesis and Monoclonal Antibody Binding Studies Using the X-ray Structure of Mac-2 Binding Protein and a Molecular Model of the CD6 Ligand Binding Domain

Jürgen Bajorath[1,2]

[1]New Chemical Entities, Inc. (NCE), 18804 North Creek Pkwy. S., Bothell, WA 98011-8805, USA. Tel: (425) 424-7297; Fax: (425) 424-7299; E-mail: jbajorath@nce-mail.com

[2]Department of Biological Structure, University of Washington, Seattle, WA 98194, USA.

Received: 27 September 1999/ Accepted: 05 November 1999/ Published: 19 November 1999

Abstract The extracellular region of CD6 consists of three scavenger receptor cysteine-rich (SRCR) domains and binds activated leukocyte cell adhesion molecule (ALCAM), a member of the immunoglobulin superfamily (IgSF). Residues important for the CD6-ALCAM interaction have previously been identified by mutagenesis. A total of 22 CD6 residues were classified according to their importance for anti-CD6 monoclonal antibody (mAb) and/or ALCAM binding. The three-dimensional structure of the SRCR domain of Mac-2 binding protein has recently been determined, providing a structural prototype for the SRCR protein superfamily. This has made a thorough three-dimensional analysis of CD6 mutagenesis and mAb binding experiments possible. Mutation of buried residues compromised both mAb and ALCAM binding, consistent with the presence of structural perturbations. However, several residues whose mutation affected both mAb and ALCAM binding or, alternatively, only ligand binding were found to map to the surface in the same region of the domain. This suggests that the CD6 ligand binding site and epitopes of tested mAbs overlap and provides an explanation for the finding that these mAbs effectively block ALCAM binding. An approximate molecular model of CD6 was used to delineate the ALCAM binding site.

Keywords Binding site, Critical residues, Crystal structure, Model building, Monoclonal antibodies, Mutagenesis, Receptor-ligand interactions

Abbreviations ALCAM, activated leukocyte cell adhesion molecule; CD6D3, third (membrane-proximal) extracellular domain of CD6; IgSF, immunoglobulin superfamily; mAb, monoclonal antibody; M2BP, Mac-2 binding protein; SRCR, scavenger receptor cysteine-rich domain; SRCRSF, scavenger receptor cysteine-rich protein superfamily

Introduction

CD6 is a cell surface receptor expressed on mature T cells, some B cells, and in the brain [1,2]. It is thought to play a role in T cell activation as a costimulatory/accessory molecule [2,3]. CD6 is a member of the scavenger receptor cysteine-rich (SRCR) protein superfamily (SRCRSF) [4], named after a characteristic C-terminal domain found in the type I macrophage scavenger receptor [5]. The SRCRSF includes a number of leukocyte antigens, for example, CD5 and CD6, but also proteins from primitive organisms, for example, the sea urchin speract receptor [2,4]. Extracellular segments of SRCRSF proteins consist of a varying number of SRCR domains [2]. The extracellular region of CD6 has three such domains, each having approximately 100 residues [1,2]. CD6 recognizes activated leukocyte cell adhesion molecule (ALCAM) [6,7], a type I transmembrane protein belonging to the immunoglobulin (Ig) superfamily (IgSF) [8], and also binds the chicken neural adhesion molecule BEN/DM-GRASP [9], an ALCAM homologue [10]. At present, the CD6-ALCAM interaction, as further described below, is the most extensively characterized interaction involving a receptor belonging to the SRCRSF, for which ligands have been difficult to identify [2].

The extracellular region of ALCAM consists of five Ig domains [7], two variable-type followed by three constant-like domains [8]. Binding experiments with different recombinant forms of CD6 and ALCAM have shown that the third (membrane-proximal) SRCR domain of CD6 (CD6D3) specifically binds the N-terminal Ig domain of ALCAM and that other domains are not required for the interaction [11,12]. Neither the first nor the second SRCR domain of CD6 bind ALCAM. The binding domains of CD6 and ALCAM from man and mouse display cross-species interactions [12,13]. Mutagenesis of ALCAM has shown that residues important for CD6 binding map to one face of the Ig-domain [14-16] that is conserved in mouse and human ALCAM [13,14].

CD6D3 has also been tested by site-directed mutagenesis in order to identify residues important for ALCAM binding [17,18]. In the absence of any knowledge about the three-dimensional (3D) structure of SRCR domains, residues were selected for mutagenesis on the basis of SRCRSF sequence comparison [17] and mutants were tested for binding to ALCAM and conformationally sensitive mAbs. On the basis of these binding profiles, 22 residues could be classified according to their importance for mAb and/or ligand binding [18]. Three residues, whose mutation only affected ALCAM binding, were considered critical for ligand recognition. The interpretation of mutagenesis and binding data was necessarily limited, since no 3D structure of CD6 or any other SRCR domain was available.

Recently, the structure of the SRCR domain of human Mac-2 binding protein (M2BP) [19,20] has been determined by X-ray crystallography [21], providing a first structural prototype for the SRCRSF. Sequence comparison in light of the M2BP structure suggested that this structure represents the canonical fold of many SRCR domains including CD6 [21]. Accordingly, M2BP has been used here as a structural template to evaluate the results of CD6D3 mutagenesis stud-

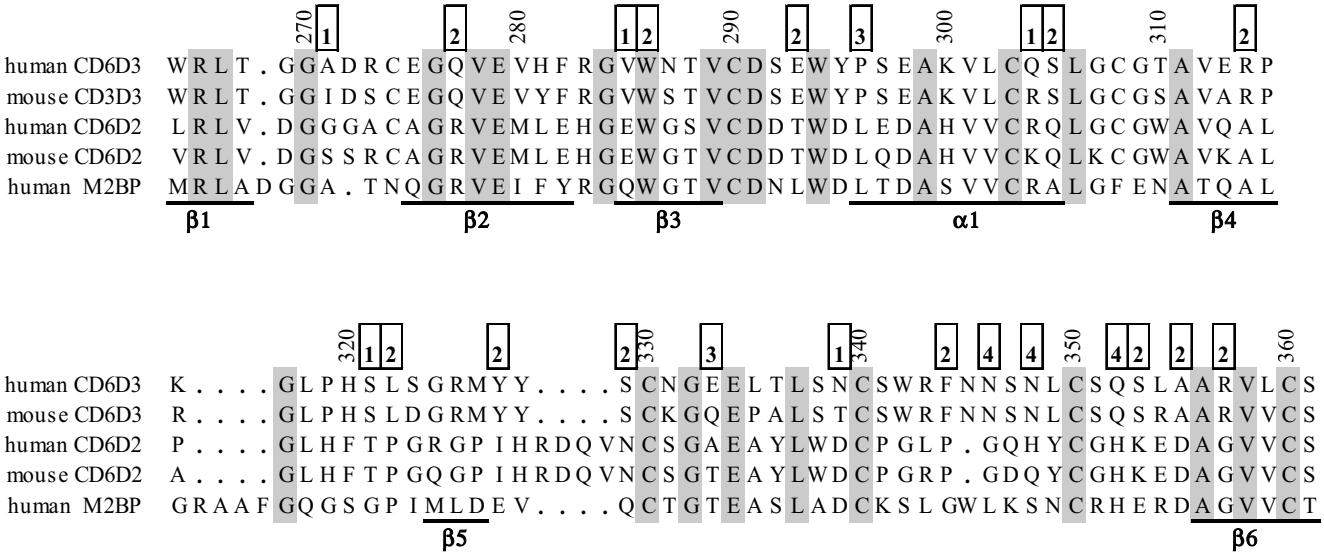

Figure 1 ***Alignment of SRCR domains in CD6 and M2BP.*** *Human and mouse CD6 domains 2 (CD6D2) and 3 (CD6D3) were aligned with M2BP. Residue numbers are given for human CD6. Conserved residues are shaded. Secondary structure elements in M2BP are underlined and labeled. CD6D1 displays a long insertion in the β4-β5 loop relative to other CD6 domains and was omitted for clarity. Mutated human CD6D3 residues are shown with boxes reporting its classification (1-4): Mutation did not affect mAb or ligand binding (1), reduced or abolished both mAb and ligand binding (2), compromised mAb but not ligand binding (3), or disrupted ligand but not mAb binding (4).*

ies. This analysis has greatly improved the ability to understand mAb and ligand binding data obtained for a variety of CD6D3 mutants and to identify residues important for the CD6-ligand interaction. Mutation of CD6D3 residues that correspond to buried, or partially buried, positions in M2BP always disrupted mAb and ligand binding. However, several CD6D3 residues that, when mutated, also compromised mAb and ligand binding map to surface exposed positions close to residues whose mutation affected only ALCAM binding. This suggests that these mutants directly compromised mAb and ALCAM binding, rather than grossly perturbing the 3D structure of CD6D3. Thus, the structure-aided analysis of mutagenesis data implicated an extended set of CD6D3 residues in ALCAM binding. These findings have made it possible to delineate the CD6 ligand binding site and analyze its spatial relation to mAb epitopes.

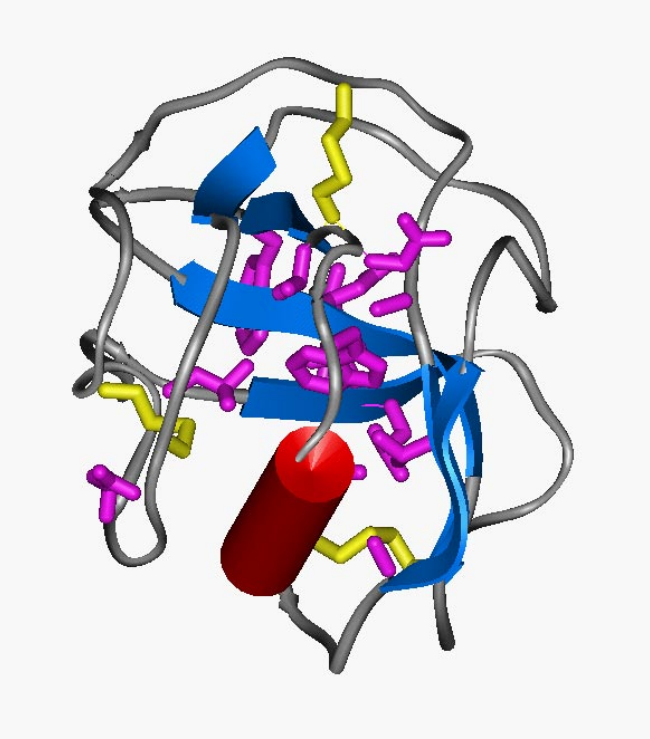

Figure 2 ***SRCR domain structure.*** *A schematic representation of M2BP is shown (α-helix, red cylinder; β-strands, blue flat ribbons; β-turns, loops, and regions of non-α or -β structure, silver). Side chains of residues that are conserved in CD6 are colored magenta, except cysteine residues (shown in yellow). The majority of these residues participate in the formation of the hydrophobic core. Secondary structure elements were defined according to Kabsch and Sander [35]. In this orientation, the extended region of non-classical secondary structure (see text) is at the top and the N- and C-termini are at the bottom of the domain.*

Methods

Coordinates of the M2BP SRCR domain are available from the Brookhaven Protein Data Bank (PDB) [22] (entry 1by2). CD6 sequences were obtained from the SWISS-PROT data bank [23] (human CD6, entry P30203) and GenBank [24] (mouse CD6, entry U37544) and aligned using the sequence-structure alignment function of MOE [25]. The alignment was manually modified to match corresponding residue positions in M2BP and CD6. Computer graphical analysis of the M2BP structure and residue mapping studies were carried out with MOE and WebLab Viewer Lite [26]. Backbone segments conserved in M2BP and CD6D3 were assembled to provide the core of a CD6D3 molecular model. Side chain replacements [27] and non-conserved segments in CD6D3 were modeled using the MOE-Homology module that combines features of α-carbon distance matrix [28] and segment matching [29] techniques to extract suitable fragments from PDB structures. The CD6D3 model, consisting of 97 residues (265-361), was energy minimized using the MOE force field [30] and complete hydrogen atom representation (following energy minimization, hydrogen atoms were removed). Only partial minimization was carried out (i.e., until the root mean square (rms) derivative of the energy function was less than 1 kcal/mol/Å) to refine intramolecular contacts but avoid substantial departures from the X-ray template (e.g., more than 1 Å α-carbon rms deviation). The model displayed reasonable stereochemistry and contacts, as assessed with PROCHECK [31]. Using ALIGN [32], 94 of 97 residues in the CD6D3 model could be superposed on corresponding positions in M2BP with an α-carbon rms deviation of 0.74 Å.

Results and discussion

SRCR domain fold and sequences

Figure 1 shows a structure-oriented alignment of SRCR domain sequences of M2BP and CD6, highlighting M2BP secondary structure elements and conserved residues. The M2BP and CD6 sequences are approximately 30% identical. Figure 2 shows a schematic representation of the M2BP structure. M2BP is a compactly folded module with a central curved β-sheet packing against an α-helix. The sheet-helix interface includes several residues that participate in the formation of the hydrophobic core of the domain. The majority of hydrophobic core residues are conserved in CD6 and other SRCRSF proteins [21]. The presence of three conserved disulfide bonds, as seen in M2BP, is a characteristic feature of SRCRSF proteins belonging to subgroup A [2,4]. Members of subgroup B, to which CD6 belongs, usually have an additional conserved disulfide bond. Cysteine residues forming this bond in CD6D3 correspond to residues N15 and F49 in M2BP whose α-carbon positions are approximately 7 Å apart. Thus, the formation of this disulfide bond is consistent with the M2BP structure [21]. The conservation of disulfide

bonds and other hydrophobic core residues leaves little doubt that M2BP represents a canonical fold for proteins belonging to the SRCRSF. M2BP displays an extended region of non-regular secondary structure between strands β5 and β6, shown at the top of Figure 2 (see also Figure 1), that is disulfide-linked to the core of the domain. As discussed below, the corresponding region in CD6D3 contains residues important for ligand binding.

Variable regions in M2BP and CD6D3

At least three segments in M2BP are not conserved in CD6D3. These segments include the β1-β2 loop, a four residue deletion in CD6D3 relative to M2BP between β4 and residue C330, and the region between C340 and β6, which corresponds to the extended segment of non-classical secondary structure (Figure 1). In the sequence alignment, the four residue deletion in CD6D3 was accommodated in the turn following β4 but CD6D3 residues in this and the subsequent region, including β5, could not be unambiguously aligned with M2BP. Thus, mapping of CD6D3 residues to corresponding positions in this region of M2BP was approximate.

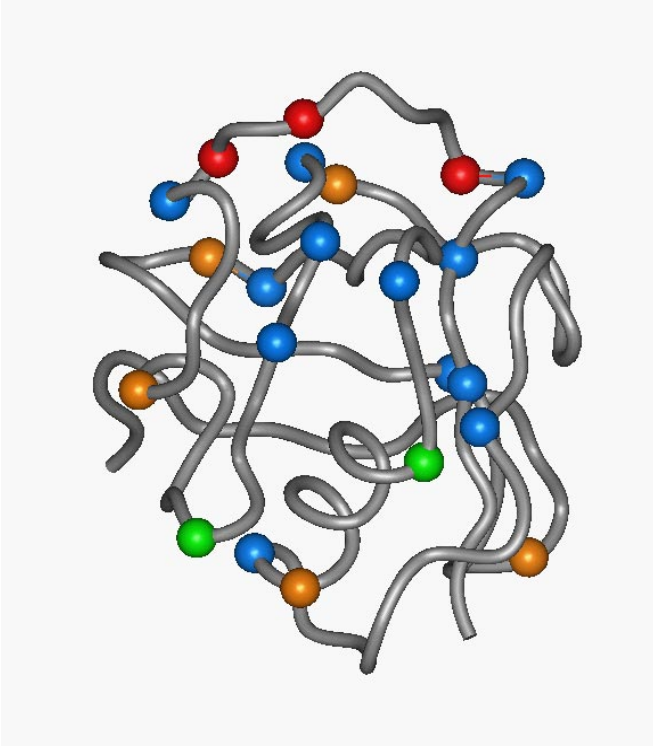

Figure 3 ***Mapping of mutated CD6D3 residues.*** *CD6D3 residues targeted by mutagenesis were mapped to corresponding positions of the M2BP structure (shown as a solid ribbon). The orientation of the view is similar to Figure 2. The α–carbon atoms of targeted positions are depicted as spheres and color-coded according to the classification reported in Figure 1 and discussed in the text: Class 1, gold; class 2, blue; class 3, green; class 4, red.*

CD6D3 mutagenesis strategy

In the following, the previously applied mutagenesis strategy [17,18] is briefly described. Residues distributed over the entire sequence of CD6D3 were tested by site-directed mutagenesis. Since CD6 displays cross-species ligand binding [12,13], the majority of selected residues were conserved in human and mouse CD6D3 but not in other SRCR domains. By contrast, residues conserved in many different SRCR domains were not mutated, as these residues were thought to play structural rather than functional roles. Selected residues were mutated to arginine or glutamic acid (e.g., A271 to R, R283 to E). These drastic changes were carried out to measurably affect 3D structural integrity and/or ligand binding. A total of 31 site-specific CD6D3 mutants were constructed, and 27 mutant proteins could be transiently expressed as Ig-fusion proteins in COS cells in sufficient quantities for further characterization. These mutant proteins were tested for binding to ALCAM and a panel of four conformationally sensitive anti-CD6D3 mAbs. Conformationally sensitive mAbs were identified by their inability to bind CD6D3 in Western blots under denaturing conditions. Mutation of any of three residues in the C-terminal region of CD6D3 (N346, N348, Q352) disrupted ALCAM but not mAb binding, suggesting that these residues were important for ligand recognition. However, mutation of 14 residues affected mAb binding, at varying levels, indicating that these changes either compromised CD6D3 structural integrity or, alternatively, disrupted mAb epitopes.

Classification of mutated CD6D3 residues

On the basis of mAb and ALCAM binding profiles [17,18], a total of 22 mutated CD6D3 residues were classified and divided into four groups. These include residues whose mutation did not affect mAb or ligand binding (class 1), reduced or abolished both mAb and ligand binding (class 2), compromised only mAb but not ligand binding (class 3), or disrupted only ligand but not mAb binding (class 4). Classifications are reported in Figure 1 and Table 1. Mutation of residues belonging to class 2 either affected both mAb and ALCAM binding directly (e.g., if exposed on the protein surface) or, alternatively, compromised the gross structural integrity of CD6D3 (e.g., if buried in the core). These alternative possibilities could not be investigated in the absence of 3D structures. Therefore, the conservative approach was to consider class 2 residues as important for structural integrity and exclude them from binding site analysis [18]. Thus, only mutants that bound at CD6D3 wild-type levels to all four mAbs were considered structurally sound. The binding profiles of residues P296 and E333 differed from other class 2 residues (and were defined here as class 3). When mutated to arginine or lysine, P296 and E333 displayed reduced or abolished bind-

Table 1 *Mapping of mutated CD6D3 residues to corresponding positions in M2BP*

Residue[a]	Class[b]	Location[c]	Likely effect of mutation[d]	Confidence[e]
A271	1	Loop: exposed	None	Low
Q277	2	α-strand: buried	Structural perturbation	High
V285	1	α-strand: exposed	None	High
W286	2	α-strand: partially buried	Structural perturbation	High
E293	2	Loop: exposed	Disrupts mAbE and LGB	High
P296	3	α-helix: exposed	Disrupts mAbE	High
Q304	1	α-helix: exposed	None	High
S305	2	α-helix: partially buried	Structural perturbation	High
R314	2	α-strand: partially buried	Structural perturbation	High
S321	1	Loop: exposed	None	Low
L322	2	Loop: partially buried	Structural perturbation	Low
Y327	2	Loop: exposed	Disrupts mAbE and LGB	Low
S329	2	Loop: exposed	Disrupts mAbE and LGB	Medium
E333	3	Loop: exposed	Disrupts mAbE	High
N339	1	Loop: exposed	None	High
F344	2	Loop: exposed	Disrupts mAbE and LGB	Medium
N346	4	Loop: exposed	Disrupts LGB	Medium
N348	4	Loop: partially buried	Disrupts LGB	Medium
Q352	4	Loop: exposed	Disrupts LGB	Medium
S353	2	Loop: exposed	Disrupts mAbE and LGB	Medium
A355	2	Loop: buried	Structural perturbation	High
R357	2	α-strand: buried	Structural perturbation	High

[a] Mutated residue in CD6D3
[b] Classification of mutated residues on the basis of mAb and ALCAM binding profiles (1: Mutation did not affect mAb or ligand binding; 2: reduced or abolished both mAb and ligand binding; 3: compromised mAb but not ligand binding; 4: disrupted ligand but not mAb binding)
[c] Corresponding residue position in M2BP; ("Loop": CD6D3 residues that map to loops, β-turns, or regions of non-classical secondary structure, "exposed": residues with side chains fully accessible on the protein surface).
[d] Prediction taking 3D analysis of residue positions and binding profiles of mutants into account ("LGB": Ligand binding; "mAbE": mAb epitopes; "None": No effect on structure, mAb, or ligand binding; "Structural perturbation": Significant perturbation of gross 3D structural integrity).
[e] Confidence level assigned to mapping of each residue ("High": Residue maps to segments conserved in CD6D3 and M2BP; "Medium": Backbone conformation is likely to differ; "Low": Conformation and local alignment of residues are ambiguous).

ing to at least two of the four mAbs but normal ALCAM binding.

Three-dimensional mapping of mutated CD6D3 residues

All 22 classified CD6D3 residues were mapped using the M2BP structure. The results are shown in Figure 3. Three of the 22 residue positions (only those important for ALCAM but not mAb binding) were previously mapped by Hohenester et al. when reporting the M2BP X-ray structure [21]. The corresponding positions are located in the extended region of non-classical secondary structure in M2BP and are shown in red at the top of Figure 3. The majority of positions where mutations affected mAb and/or ALCAM binding (blue and red) map to the upper half of the domain (as shown in Figure 3). By contrast, mutations that affected only mAb binding or do not affect binding at all (green and gold) are mostly located in the lower part. Thus, the distribution of these residues indicated that the upper part of the domain contains the CD6 ligand binding site.

Residue analysis

A detailed analysis of all 22 residue positions and putative effects of CD6D3 mutations are summarized in Table 1. Assignments have different confidence levels dependent on the location of analyzed residue positions. Residues in regions conserved in M2BP and CD6D3 can be unambiguously mapped, and thus the confidence level is high. This is not the case for residues in variable regions. For example, F344 in CD6D3 corresponds to a glycine with unusual torsion angles in M2BP and, therefore, the local backbone conformation of this region most likely differs in these proteins, making it

more difficult to accurately map the position of this residue. Therefore, in this case, the confidence level is lower. However, overall residue mapping correlates very well with observed binding profiles of CD6D3 mutants. Mutation of seven of eight residues in CD6D3 that map to buried, or partially buried, positions in M2BP displayed both reduced or abolished mAb and ligand binding. This is consistent with the idea that mutation of buried residues is likely to compromise 3D structural integrity. On the other hand, all five residues whose mutation affected neither mAb nor ALCAM binding map to surface exposed positions, where mutations are not expected to affect 3D structural integrity. One implication of these findings is that mAb binding profiles were reliable tools to monitor gross structural perturbations of mutant proteins, consistent with the results of an independent study on the human CD40 ligand [33]. Residues P296 and E333 (colored green in Figure 3), whose mutation affected mAb but not ALCAM binding also mapped to surface positions. Since these mutants bound ALCAM normally, their 3D structure was largely unperturbed. Residues P296 and E333 are close to each other on the protein surface but distant from residues only important for ALCAM binding. This is consistent with the idea that these residues are part of mAb epitopes but not the ALCAM binding site. Furthermore, five residues (E293, Y327, S329, F344, and S353) whose mutation reduced or abolished both ALCAM and mAb binding map to surface exposed (rather than buried) positions in M2BP proximal to residues whose mutation only affected ALCAM binding. These positions are shown in Figure 4.

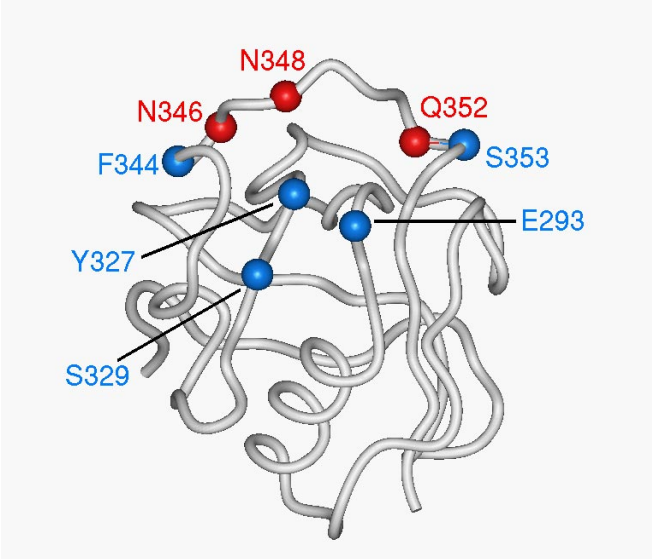

Figure 4 ***Mapping of CD6D3 residues important for binding.*** *CD6D3 residues that are important for ALCAM binding (red) or both ALCAM and mAb binding (blue) and that map to surface exposed positions in M2BP (represented as a solid ribbon) are shown. These residues cluster in the upper half of the domain. The α–carbon atoms of residue positions in M2BP are depicted as spheres and labeled with the corresponding CD6D3 residue and number. The orientation of M2BP is the same as in Figure 3.*

Residues implicated in mAb and ALCAM binding

The above residue analysis suggests that mutation of residues E293, Y327, S329, F344, or S353 did not compromise the gross structural integrity of CD6D3 but affected both mAb and ALCAM binding directly. This conclusion is based on their surface exposed location and spatial proximity to residues N346, N348, and Q352 that are important for ALCAM recognition but not mAb binding. All of these eight residues are conserved in human and mouse CD6D3, consistent with the presence of cross-species CD6-ligand binding [12,13]. However, these residues are not conserved in other CD6 SRCR domains, consistent with the finding that only CD6D3 binds ALCAM [11,12]. Since mutation of each of the five residues E293, Y327, S329, F344, and S353 affected binding of four tested mAbs, albeit at different levels [17,18], and ALCAM binding, epitopes of these mAbs not only overlap with each other but most likely also overlap with the ALCAM binding site in CD6D3. This view is consistent with the observation that these four anti-CD6D3 mAbs effectively block ALCAM binding [17,18].

ALCAM binding site in CD6D3

Taken together, these findings suggest that eight residues (E293, Y327, S329, F344, N346, N348, Q352, and S353) in three different sequence segments outline the ALCAM binding site. Therefore, a molecular model of CD6D3 was built based on the M2BP structure and the sequence alignment in Figure 1. The model provides a better approximation of the molecular surface of CD6D3 than the M2BP structure. Seven of the eight residues (except E293) map to regions that are variable in M2BP and CD6D3 and where alternative local sequence alignments are possible (as described above). Such regions are difficult to model with high confidence [33,34] and are only tentative in the CD6D3 model. Accordingly, structural details (e.g., exact residue conformations) of the ALCAM binding site in CD6 were not predicted, and the analysis was limited to providing a spatial outline using surface representations, as shown in Figure 5. Despite these limitations, general characteristics of this region can be described. Residues important for binding map to the surface and delineate a relatively flat surface area in CD6D3 that is located opposite to the N- and C-termini of the domain. Thus, the location and shape of this site are well suited to recognize the binding face [14] of the terminal Ig domain of ALCAM. Ligand binding to this region is distant from putative SRCR domain interfaces in CD6 and should thus not dependent on their structural integrity, consistent with the finding that CD6D3-Ig fusion protein binds ALCAM like wild-type CD6 [11]. An important finding is that part of the ALCAM binding site overlaps with mAb epitope regions. This explains why these mAbs effectively block ALCAM binding. Consid-

ering the spatial arrangement of residues implicated in both mAb and ALCAM binding or only in mAb binding (blue and green in Figure 5), mAbs could bind in many orientations to this site. However bound, these mAbs would directly compete and/or, due to their size, sterically interfere with ligand binding to CD6D3.

Conclusions

Analysis of CD6D3 residues in light of the X-ray structure of M2BP, a prototypic SRCR domain, has much improved the interpretation of CD6D3 mutagenesis data generated prior to the availability of an SRCR domain structure. The location of mutagenesis sites and their structural environment could be correlated with mAb and ligand binding profiles of CD6D3 mutant proteins. This has made it possible to identify an extended set of CD6D3 residues implicated in binding and, with the aid of a molecular model of CD6D3, the ALCAM binding site could be located and compared to mAb epitope regions. The analysis illustrates the importance of 3D structural data for the design and rationalization of mutagenesis experiments. The location of the ALCAM binding site in CD6D3 and the sequence variability of this region in SRCR domains of CD6, M2BP, and other members of this protein family suggest that other SRCRSF receptors may utilize corresponding regions for specific recognition of ligands.

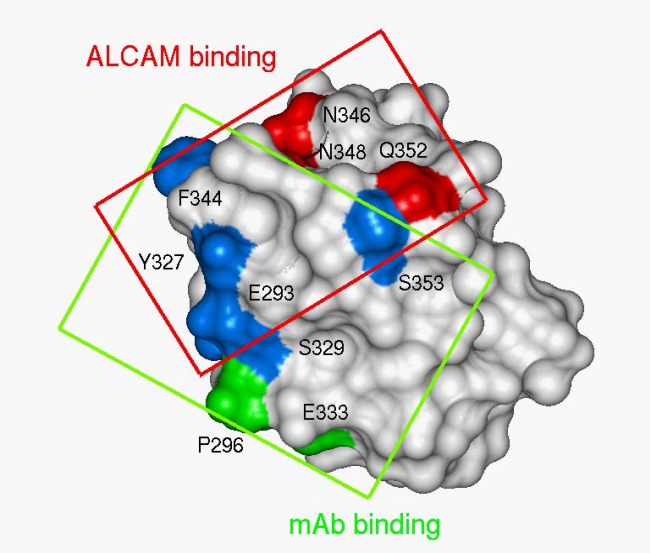

Figure 5 ***Outline of the ALCAM binding site in CD6D3.*** *The CD6D3 model is shown with solvent-accessible surface [36] (2.0 Å probe radius). Residues important for ALCAM and/or mAb binding are color-coded according to Figure 3 (i.e., red, important only for ALCAM binding; blue, important for both ALCAM and mAb binding; green, important only for mAb binding). The model is oriented to best display residues important for binding (focusing on the top of the SRCR domain). Boxes approximately delineate mAb epitope regions (green box) and the ALCAM binding site (red), as suggested by the spatial arrangement of mutated residues and their binding profiles. The figure illustrates that the ALCAM and mAb binding sites overlap.*

Supplementary material available Coordinates of a CD6D3 molecular model are available in pdb format.

Acknowledgment The author is very grateful to Erhard Hohenester, Department of Crystallography, Birkbeck College, University of London, Malet Street, London WC1E 7HX, UK, for making coordinates of entry 1by2 available prior to official PDB release.

References

1. Aruffo, A.; Melnick, M. B.; Linsley, P. S.; Seed B. *J. Exp. Med.* **1991**, *174*, 949.
2. Aruffo, A.; Bowen, M. A.; Patel, D. D.; Haynes, B. F.; Starling, G. C.; Gebe, J. A.; Bajorath, J. *Immunol. Today* **1997**, *18*, 498.
3. Morimoto, C.; Rudd, C. E.; Letvin, N. L.; Hagan, M.; Schlossman, S. F. *J. Immunol.* **1988**, *140*, 2165.
4. Resnick, D.; Pearson, A.; Krieger, M. *Trends Biochem. Sci.* **1994**, *19*, 5.
5. Kodama, T.; Freeman, L.; Rohrer, J.; Zabrecky, J.; Matsudaira, P.; Krieger, M. *Nature* **1990**, *343*, 531.
6. Patel, D. D.; Wee, S.-F.; Whichard, L. P.; Bowen, M. A.; Pesando, J. M.; Aruffo, A.; Haynes, B. F. *J. Exp. Med.* **1994**, *181*, 1563.
7. Bowen, M. A.; Patel, D. D.; Li, X.; Modrell, B.; Malacko, A. R.; Wang, W.-C.; Marquardt, H.; Neubauer, M.; Pesando, J. M.; Francke, U.; Haynes, B. F.; Aruffo, A. *J. Exp. Med.* **1995**, *181*, 2213.
8. Williams, A. F.; Barclay, A. N. *Ann. Rev. Immunol.* **1988**, *6*, 381.
9. Skonier, J. E.; Bowen, M. A.; Aruffo, A.; Bajorath, J. *Protein Sci.* **1997**, *6*, 1768.
10. Burns, F. R.; von Kannen, S.; Guy, L.; Raper, A.; Kamholz, J.; Chang, S. *Neuron* **1991**, *7*, 209.
11. Bowen, M. A.; Bajorath, J.; Siadak, A. W.; Modrell, B.; Malacko, A. R.; Marquardt, H.; Nadler, S. G.; Aruffo, A. *J. Biol. Chem.* **1996**, *271*, 17390.
12. Whitney, G. S.; Starling, G. C.; Bowen, M. A.; Modrell, B.; Siadak, A. W.; Aruffo, A. *J. Biol. Chem.* **1995**, *270*, 18190.
13. Bowen, M. A.; Bajorath, J.; D'Egidio, M.; Whitney, G. S.; Palmer, D.; Kobarg, J.; Starling, G. C.; Siadak, A. W.; Aruffo, A. *Eur. J. Immunol.* **1997**, *27*, 1469.
14. Skonier, J. E.; Bowen, M. A.; Emswiler, J.; Aruffo, A.; Bajorath, J. *Biochemistry* **1996**, *35*, 12287.
15. Skonier, J. E.; Bowen, M. A.; Emswiler, J.; Aruffo, A.; Bajorath, J. *Biochemistry* **1996**, *35*, 14743.
16. Bajorath, J.; Bowen, M. A.; Aruffo, A. *Protein Sci* **1995**, *4*, 1644.

17. Bodian, D. L.; Skonier, J. E.; Bowen, M. A.; Neubauer, M.; Siadak, A. W.; Aruffo, A.; Bajorath, J. *Biochemistry* **1997**, *36*, 2637.
18. Skonier, J. E.; Bodian, D. L.; Emswiler, J.; Bowen, M. A.; Aruffo, A.; Bajorath, J. *Protein. Eng.* **1997**, *10*, 943.
19. Iacobelli, S.; Arno, E.; D'Orazio, A.; Coletti, G. *Cancer Res.* **1986**, *46*, 3005.
20. Tinari, N.; D'Egidio, M.; Iacobelli, S.; Bowen, M.; Starling, G. C.; Seachord, C.; Darveau, R. P.; Aruffo, A. *Biochem. Biophys. Res. Commun.* **1997**, *232*, 367.
21. Hohenester, E.; Sasaki, T.; Timpl, R. *Nature Struct. Biol.* **1999**, *6*, 228.
22. Bernstein, F. C.; Koetzle, T. F.; Williams, G. J.; Meyer, Jr. E. E.; Brice, M. D.; Rodgers, J. R.; Kennard, O.; Shimanouchi, T.; Tasumi, M. *J. Mol. Biol.* **1977**, *112*, 535.
23. Bairoch, A.; Apwiler, R. *Nucl. Acid Res.* **1999**, *27*, 49.
24. Benson, D. A.; Boguski, M. S.; Lipman, D. J.; Ostell, J.; Ouellette, B. F. *Nucl. Acid Res.* **1998**, *26*, 1.
25. MOE, Molecular Operating Environment, Version 1999.05, Chemical Computing Group, Inc., 1255 University Street, Suite 1600, Montreal, Quebec, Canada, H3B, 3X3. http://www.chemcomp.com
26. WebLab Viewer Lite, 1999, MSI, 9685 Scranton Road, San Diego, California, USA. http://www.msi.com/solutions/products/weblab/viewer
27. Ponder, J. W.; Richards, F. M. *J. Mol. Biol.* **1987**, *193*, 775.
28. Jones, T. A.; Thirup, S. *EMBO J.* **1986**, *5*, 819.
29. Levitt, M. *J. Mol. Biol.* **1992**, *226*, 507.
30. Labute, P. MOE Forcefield Facilities. http://www.chemcomp.com/article/ff.htm. Chemical Computing Group, Chemical Computing Group, Inc., 1255 University Street, Suite 1600, Montreal, Quebec, Canada, H3B, 3X3.
31. Laskowski, R. A.; MacArthur, M. S.; Moss, D. S.; Thornton, J. M. *J. Appl. Cryst.* **1997**, *26*, 283.
32. Satow, Y.; Cohen, G. H.; Padlan, E. A.; Davies, D. R. *J. Mol. Biol.* **1986**, *190*, 593.
33. Bajorath, J. *J. Biol. Chem.* **1998**, *273*, 24609.
34. Bajorath, J. *J. Mol. Model.* **1997**, *3*, 216.
35. Kabsch, W.; Sander, C. *Biopolymers* **1983**, *22*, 2577.
36. Connolly, M. L. *Science* **1983**, *221*, 709.